# Stereodynamics from the Stereodirected Representation of the Exact Quantum S Matrix: The Li + HF → LiF + H Reaction

**ARTICLE** *in* THE JOURNAL OF PHYSICAL CHEMISTRY · NOVEMBER 1998

DOI: 10.1021/jp982434a



**6 AUTHORS**, INCLUDING:

Vincenzo Aquilanti
Università degli Studi di Perugia
**315** PUBLICATIONS **6,407** CITATIONS
SEE PROFILE

Simonetta Cavalli
Italian National Research Council
**119** PUBLICATIONS **2,889** CITATIONS
SEE PROFILE

A. Laganà
Università degli Studi di Perugia
**162** PUBLICATIONS **2,213** CITATIONS
SEE PROFILE

Todd J. Martinez
Stanford University
**239** PUBLICATIONS **7,863** CITATIONS
SEE PROFILE

# Stereodynamics from the Stereodirected Representation of the Exact Quantum S Matrix: The Li + HF → LiF + H Reaction

**J. M. Alvariño,* V. Aquilanti, S. Cavalli, S. Crocchianti, A. Laganà, and T. Martinez†**

*Dipartimento di Chimica, Università di Perugia, 06123 Perugia, Italy*

*Received: June 1, 1998; In Final Form: September 9, 1998*

In order to investigate the stereodynamics of the Li + HF → LiF + H reaction, the exact quantum mechanical scattering matrix calculated in the $|jl\rangle$ (orbital) representation in the total energy range from 0.45 to 0.54 eV is converted into the stereodirected representation (*J. Phys. Chem.* **1991**, *95,* 8184) by an orthogonal transformation. Using total angular momentum $J = 0$ results, the dependence of the reaction probability matrix on the relative orientation of both the reactant and product molecules as well as on the direction of attack and recoil velocity is illustrated and discussed. Formulas are given, relating the exact quantum mechanical stereodynamic properties obtained from both the $|j\Omega\rangle$ (helicity) and $|\nu\Omega\rangle$ (stereodirected) representations of the scattering matrix to the information derived from classical trajectory studies and from experimentally observable polarization parameters.

## I. Introduction

The class of reactions between metal atoms and halogen-containing molecules has received wide attention, both from experimentalists and from theoreticians. In particular, the simplest example

$$\mathrm{Li}(^2\mathrm{S}) + \mathrm{HF}(^1\Sigma^+) \rightarrow \mathrm{LiF}(^1\Sigma^+) + \mathrm{H}(^2\mathrm{S}) \qquad (1)$$

is an ideal prototype for investigating the properties of asymmetric A + BC reactive systems. A hyperspherical view of the potential energy surface for this reaction, as used in calculations discussed in this paper, is shown in Figure 1.[1] Scalar properties of reaction 1, such as state-to-state probabilities, integral cross sections, and rate constants, have been successfully investigated both experimentally (using crossed molecular beam[2,3] techniques) and theoretically (using statistical,[4] quasi-classical,[5−11] approximate quantum,[12,13] and more recently, accurate quantum 3D time-dependent[14] and time-independent[15,16] techniques). Such an enormous amount of dynamical work made use of potential energy surfaces[16−19] fitted to the ab initio potential energy values computed by Chen and Schaefer[20] and others.[19] An alternative surface has been proposed and used to compute reactive scattering properties.[21]

More recently, experiments (thanks to the use of molecular beam techniques without and with polarized lasers and electric and magnetic fields[22]) have evolved in a way that studies of reaction stereodynamics (RSD) have become feasible. RSD focuses on vector properties (such as angular momentum vector correlations and a quantitative research of the *steric effect)* of the reactive process as opposed to scalar quantities (such as the selective partition of the reactant energy among product channels).

Classical trajectory studies of reaction 1 have already tackled in the past the problem of understanding RSD effects.[23] Our present goal is to calculate exact 3D values of stereodynamic properties of the Li + HF reaction starting from the recently reported accurate quantum results,[15,16,24] which, being based on a time-independent hyperspherical coordinate method, give the full **S** matrix for the process (differently from time-dependent approaches).

Seminal papers on both experimental and theoretical aspects on the general topic of vector correlations and reaction dynamics stem from Herschbach's group in the 70's (starting with refs 25 and 26). The whole topic of stereodynamics in bimolecular reactions has been the object of many recent reviews; see, for example, ref 27. For recent progress, see ref 28.

The scheme of this paper is as follows. In section II alternative **S** matrix representations and orthogonal transformations among them are described. In section III stereodynamical information that can be derived from stereodirected representations is discussed. In section IV the steric effect calculated for the Li + HF reaction is presented and analyzed. The appendix section briefly summarizes the stereodynamical information contained in the helicity representation according to the viewpoint presented in this paper.

## II. Alternative S Matrix Representations

In principle, accurate quantum mechanical calculations provide a comprehensive picture of the molecular dynamics and a rigorous description of reactive and nonreactive events. The scattering matrix **S** incorporates, in fact, all the differences between the wave function of a system experiencing the atom−molecule interaction during the collision and the unperturbed one. Asymptotically, when the atom−molecule potential is negligible, $j$ (the diatomic rotational) and $l$ (the atom−diatom orbital) angular momentum quantum numbers of the space-fixed (SF) representation are conserved (they are in this limit good quantum numbers). Together with the total angular momentum quantum number $J$ **(J = j + l)** and its projection $M$, they can be used to label the quantum states of the system and, as a consequence, the **S** matrix of the process. In the exact quantum mechanical approach, numerical procedures are used to compute an **S** matrix in the $|JMjl\rangle$ representation. In the following, the

* Permanent address: Departamento de Química Física, Universidad de Salamanca, 37008 Salamanca, Spain.

† Permanent address: Departamento de Máquinas y Motores Térmicos, Universidad del Pais Vasco, 48012 Bilbao, Spain.

10.1021/jp982434a CCC: $15.00 
Published on Web 11/03/1998

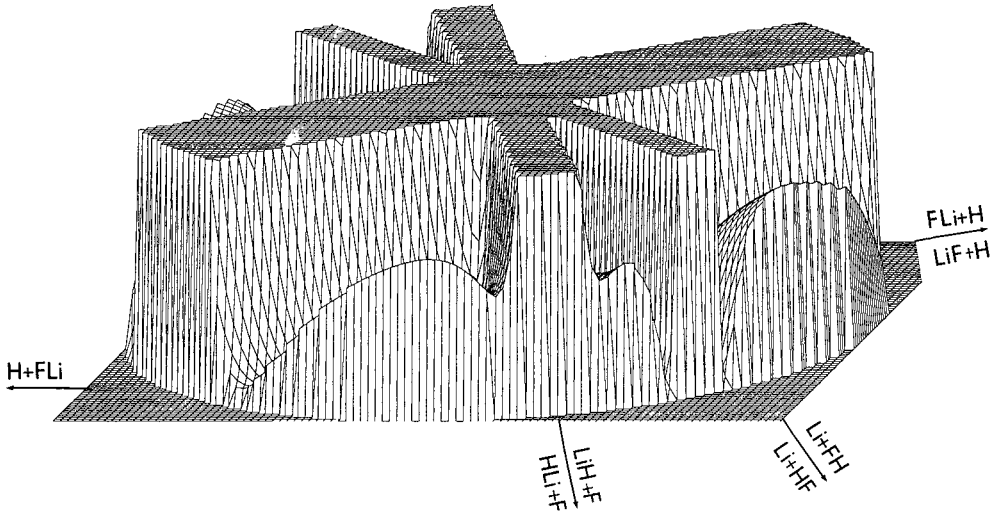


**Figure 1.** Hyperspherical perspective for the potential energy surface of the Li + HF reaction as adapted from ref 1. This is a view of the collinear configuration.

shorter notation $|jl\rangle$ will be used. Elastic, inelastic, and reactive probabilities are then obtained by proper sums over the **S** matrix elements.

Although all the information (including the stereodynamical one) is fully contained in the $|jl\rangle$ representation of the **S** matrix, other representations of the scattering matrix are more suitable for carrying out RSD studies. In this perspective, body-fixed (BF) representations are particularly useful. These representations take a particular vector of the considered arrangement as the quantization axis. We will use unprimed and primed symbols for denoting quantities referring respectively to the reactant or to the product arrangement. If the chosen vector is $\mathbf{R}_\tau$ (the atom−diatom Jacobi vector pointing from the diatom center of mass onto the atom in the reactant arrangement), the quantum number of the common projection of **J** and $\mathbf{j}_\tau$, on $\mathbf{R}_\tau$, is $\Omega$ (the projection of $\mathbf{l}_\tau$ is necessarily zero). When choosing $\mathbf{r}_\tau$ as a quantization vector (the diatom Jacobi vector pointing from the first to the second atom of the diatom in the reactant arrangement), the quantum number of the common **J** and $\mathbf{l}_\tau$, projection is $\Lambda$ (while now the projection of $\mathbf{j}_\tau$ is zero). The corresponding $|JMj\Omega\rangle$ (shortly $|j\Omega\rangle$) and $|JMl\Lambda\rangle$ (shortly $|l\Lambda\rangle$) bases can be used to represent the **S** matrix. These representations are related among themselves and the $|jl\rangle$ one by orthogonal transformations.[29,30]

An alternative exact label for the basis is the *steric quantum number* $\nu$, the projection of an artificial vector **A** precessing around $\mathbf{R}_\tau$.[31] In this case, when the modulus of this vector increases, the grid of discrete values of the precession angle more finely scans the angle $\Theta_\tau^R$ (the angle formed by the vectors $\mathbf{R}_\tau$ and $\mathbf{r}_\tau$). This representation $|JM\nu\Omega\rangle$ (shortly $|\nu\Omega\rangle$) (and its analogue $|JM\nu\Lambda\rangle$ (shortly $|\nu\Lambda\rangle$), when the precession occurs around $\mathbf{r}_\tau$**)** is obtained by orthogonal transformations from the other.

Orthogonal transformations of the **S** matrix have been discussed in detail in ref 30. Among those given there, we consider explicitly the SF to BF helicity ($|jl\rangle \rightarrow |j\Omega\rangle$) and the BF helicity → BF stereodirected $|j\Omega\rangle \rightarrow |\nu\Omega\rangle$ transformations that are needed in the following. The $|jl\rangle \rightarrow |j\Omega\rangle$ orthogonal transformation is

$$S^{J,p}_{\tau j\Omega\nu,\tau' j'\Omega'\nu'} = \sum_{ll'} G^{J,p,j}_{l\Omega} S^{J,p}_{\tau jl\nu,\tau' j'\nu'} G^{J,p,j'}_{l'\Omega'} \qquad (2)$$

where the elements of the transformation matrix are

$$G^{J,p,j}_{l\Omega} = (-)^{J+\Omega}(2l+1)^{1/2}\begin{pmatrix} j & J & l \\ \Omega & -\Omega & 0 \end{pmatrix}\sqrt{\frac{2}{1+\delta_{\Omega 0}}} \qquad (3)$$

in terms of Wigner 3*j* symbols.[29] The orthonormal properties of the transformation ensure preservation of symmetry and unitarity to the **S** matrix in this representation. For the case $J = 0$, considered in this paper, the space-fixed and helicity representations coincide. For completeness, the stereodynamical information contained in the helicity representation is discussed in the appendix section.

The $|j\Omega\rangle \rightarrow |\nu\Omega\rangle$ orthogonal transformation is

$$S^{J,p}_{\tau\Omega\nu\upsilon,\tau'\Omega'\nu'\upsilon'} = \sum_{jj'} G^{j_{\max},\Omega}_{j\nu} S^{J,p}_{\tau j\Omega\nu,\tau' j'\Omega'\nu'} G^{j_{\max},\Omega'}_{j'\nu'} \qquad (4)$$

where

$$G^{j_{\max},\Omega}_{j\nu} = (-)^{[(J_{\max}+\Omega)/2]-\nu+j}(2j+1)^{1/2}\begin{pmatrix} \frac{j_{\max}-\Omega}{2} & \frac{j_{\max}+\Omega}{2} & j \\ \nu & -\nu & 0 \end{pmatrix}\sqrt{\frac{2}{1+\delta_{\nu 0}}} \qquad (5)$$

and again, the **S** matrix in this stereodirected representation continues to be symmetric and unitary. For further discussion and use of these transformations see some related papers.[32]

## III. Stereodynamical Information from Stereodirected Representation

To extract stereodynamical information from relationships given above, one needs to calculate the $\mathbf{S}^J$ matrix for all the partial waves contributing to reaction. Since *J* may become very large before partial wave convergence is reached and computations become increasingly heavier with *J* in terms of memory and CPU time, it is likely that these data will be produced in the near future only for a limited number of systems. For this reason, this investigation is focused on those individual fixed *J* representations that can supply information about RSD properties.

As already mentioned, it is straightforward to transform helicity representations of the **S** matrix into stereodirected ones. As a matter of fact, the projection quantum number $\nu$ of the stereodirected $|\nu\Omega\rangle$ representation of the **S** matrix has to be interpreted[30,33] as a quantum label

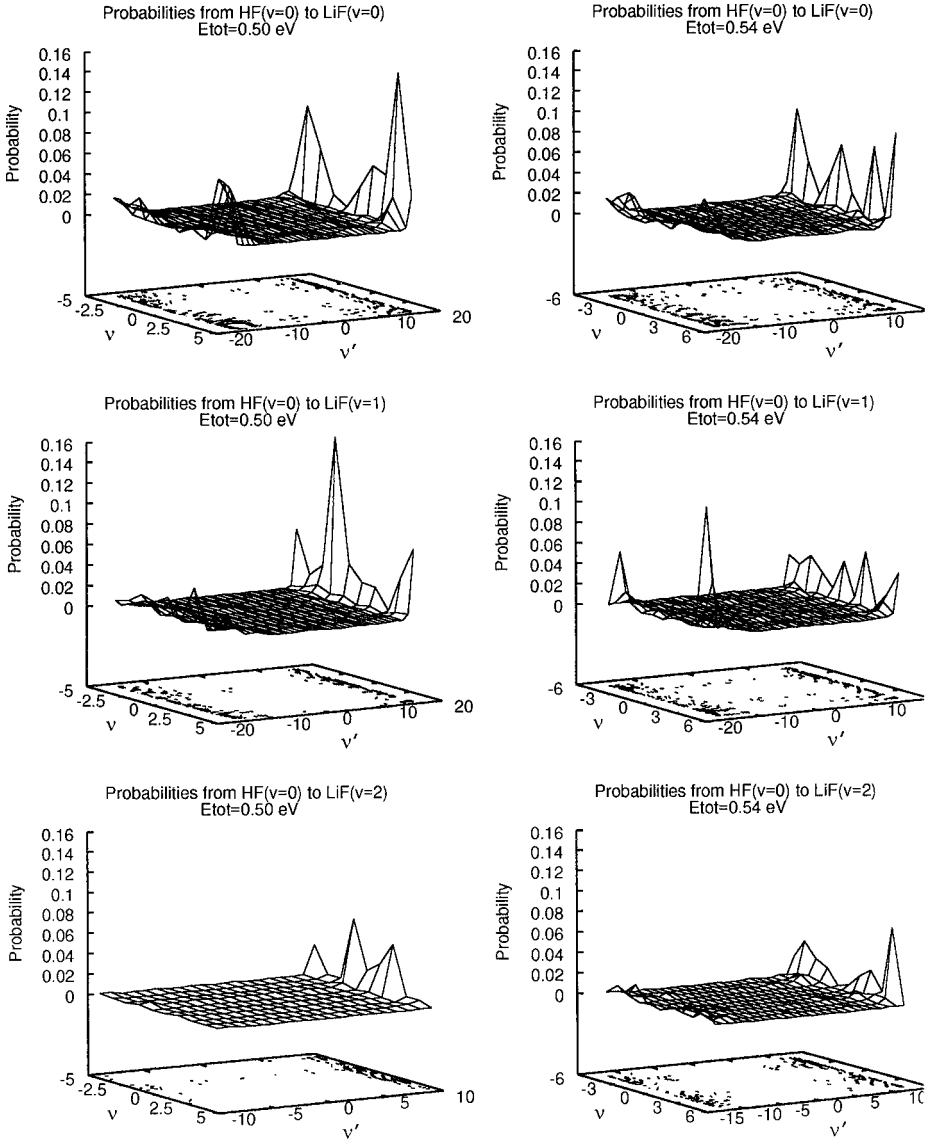


**Figure 2.** Reaction probabilities at two collision energies obtained from the scattering matrix as transformed to the stereodirected representation. Steric quantum numbers $\nu$ and $\nu'$ are for entrance (Li + HF) and exit (LiF + H) channels, respectively. Entrance channel vibrational state is $\upsilon = 0$. The three cases for exit channel vibrational states $\upsilon' = 0$, 1, and 2 are shown.

$$-\frac{j_{\max}-\Omega}{2} \le \nu \le \frac{j_{\max}-\Omega}{2} \tag{6}$$

that can be used to discretize $\Theta^R$

$$\Theta^R = \pi - \Theta^k = \arccos\left(-\frac{2\nu}{j_{\max}+1}\right) \tag{7}$$

(an analogous relationship can be established between $\nu'$ and the exit channel angle $\Theta^{R'}$).

In the case $J = 0$, one has

$$P^{J=0}_{\tau\tau'}(\nu) = \sum_{\nu'} P^{J=0}_{\tau\tau'}(\nu \rightarrow \nu') \tag{8}$$

that conveniently defines a zero total angular momentum *steric effect*.[33] It is worth pointing out here that in eq 8 the ($\upsilon \rightarrow \upsilon'$) indexes have been omitted to simplify the notation (e.g., $P^{J=0}_{\tau\tau'}(\nu)$ means $P^{J=0}_{\tau\tau'}(\nu;\upsilon\rightarrow\upsilon')$) while the $j$ and $j'$ labels disappear in the stereodirected representation. In the same equation, the probability matrix is given by

$$P^{J=0}_{\tau\tau'}(\nu \rightarrow \nu') = |S^{J=0}_{\nu\rightarrow\nu'}|^2 \tag{9}$$

In the case $J = 0$, it is also $\Omega = \Omega' = 0$ so that there is no need for summing over $\Omega$ and $\Omega'$. However, when considering $J \neq 0$, both $\Omega$ and $\Omega'$ can differ from zero, and since the range of $\nu$ values depends on $\Omega$ (see eq 6) (and the range of $\nu'$ values depends on $\Omega'$), other types of summations are of interest. In particular, the different $P^{J}_{\tau\tau'}(\nu)$ values depend parametrically on $\Omega$ (and the $P^{J}_{\tau\tau'}(\nu')$ values depend parametrically on $\Omega'$). Therefore, one has to use

$$P^{J}_{\tau\tau'}(\nu;\Omega) = \sum_{\nu',\Omega'} P^{J}_{\tau\tau'}(\Omega,\nu\rightarrow\Omega',\nu') \tag{10}$$

where $P^{J}_{\tau\tau'}(\Omega,\nu\rightarrow\Omega',\nu')$ is the probability matrix. The probability $P^{J}_{\tau\tau'}(\nu;\Omega)$ would give a fixed $J$ and fixed $\Omega$ *steric effect*, i.e., the effect of tilting the rotation plane with respect to $\mathbf{R}_\tau$ or $\mathbf{k}_\tau$ at fixed $J$ and fixed angle value.

## IV. Steric Effects for Li + HF Reaction

To examine quantum mechanically the steric effects for the Li + HF reaction, we calculated from eq 9 the detailed reactive

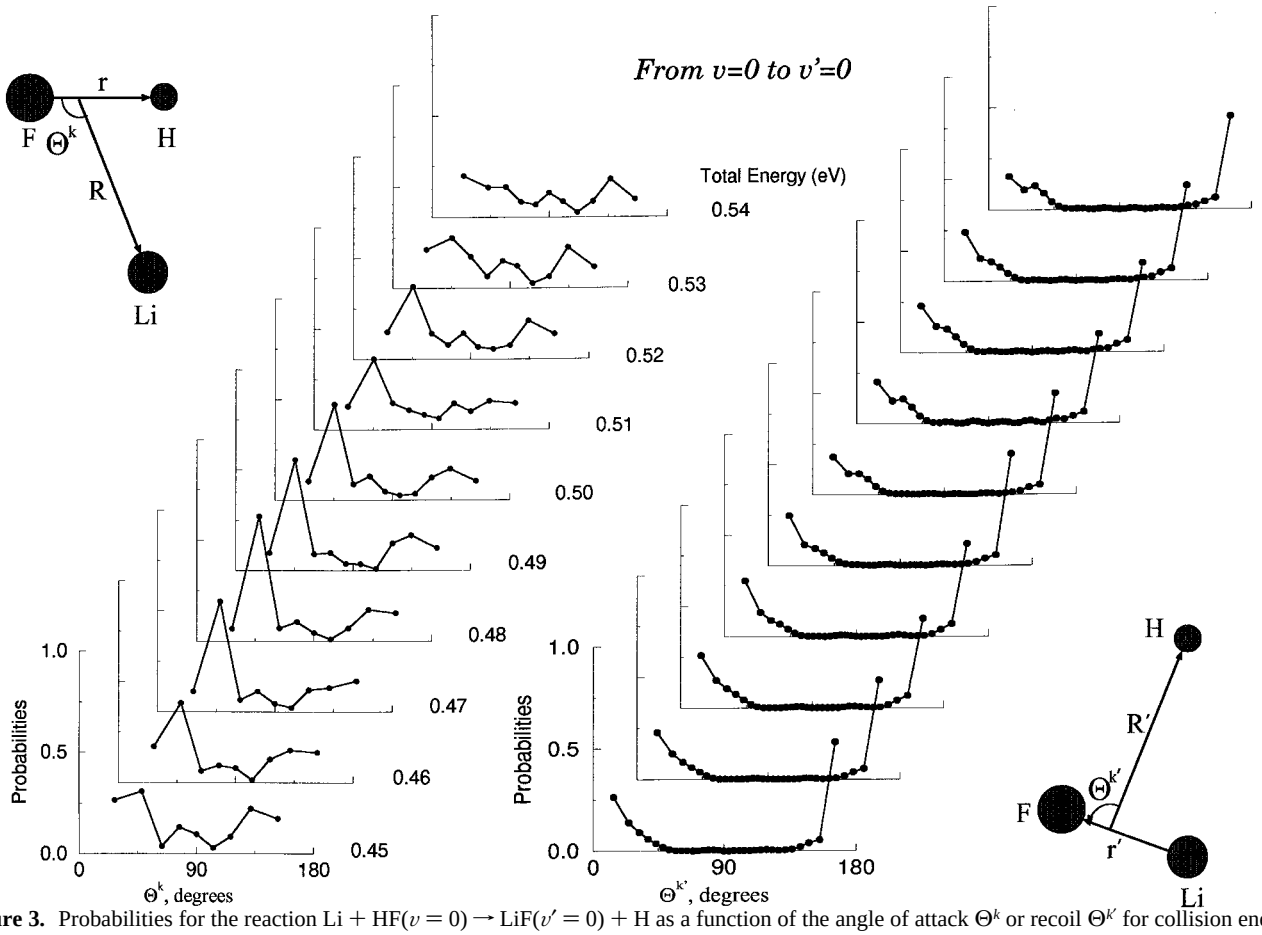


**Figure 3.** Probabilities for the reaction Li + HF($v = 0$) → LiF($v' = 0$) + H as a function of the angle of attack $\Theta^k$ or recoil $\Theta^{k'}$ for collision energy values ranging from 0.45 eV (bottom panel) to 0.54 eV (top panel).

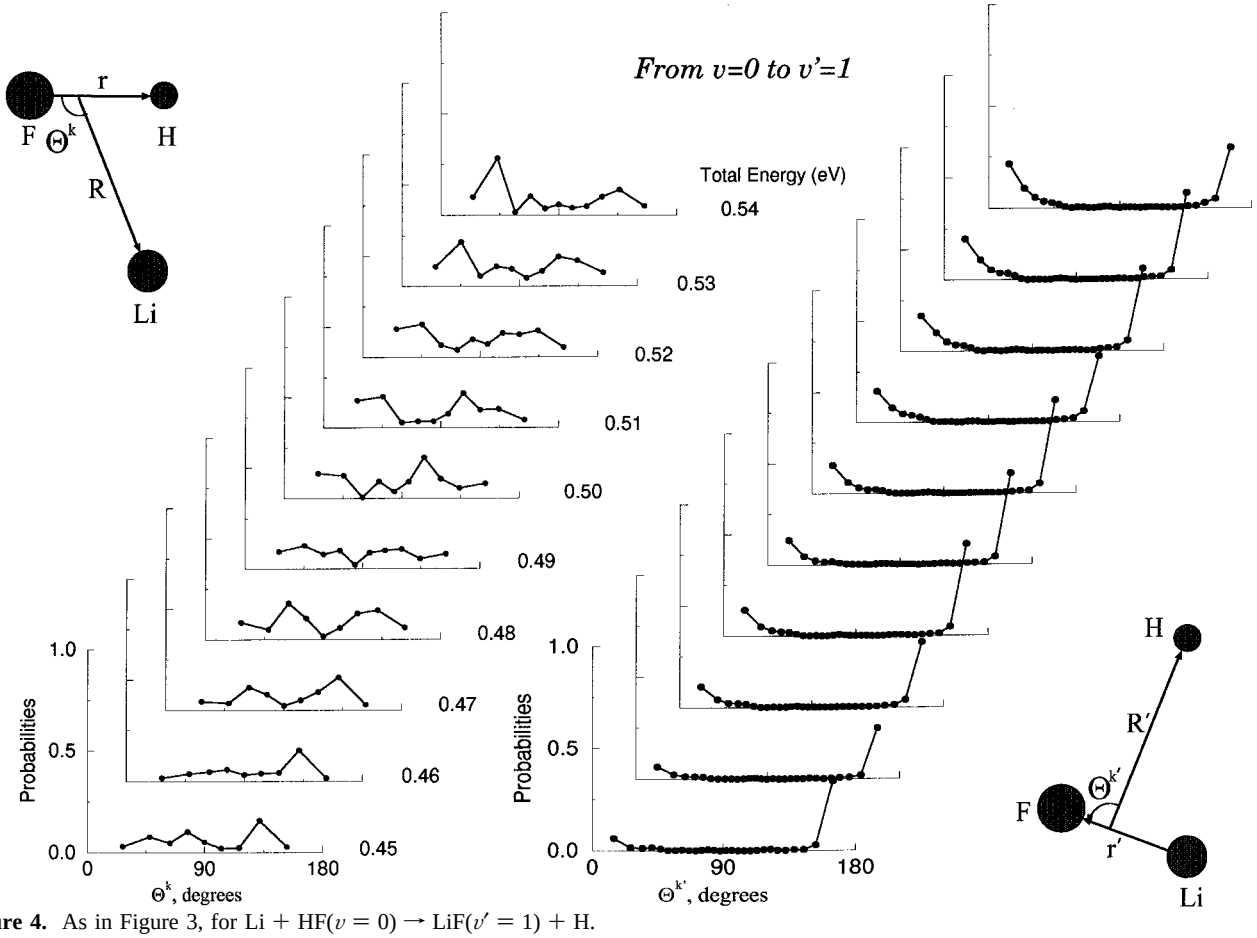


**Figure 4.** As in Figure 3, for Li + HF($v = 0$) → LiF($v' = 1$) + H.

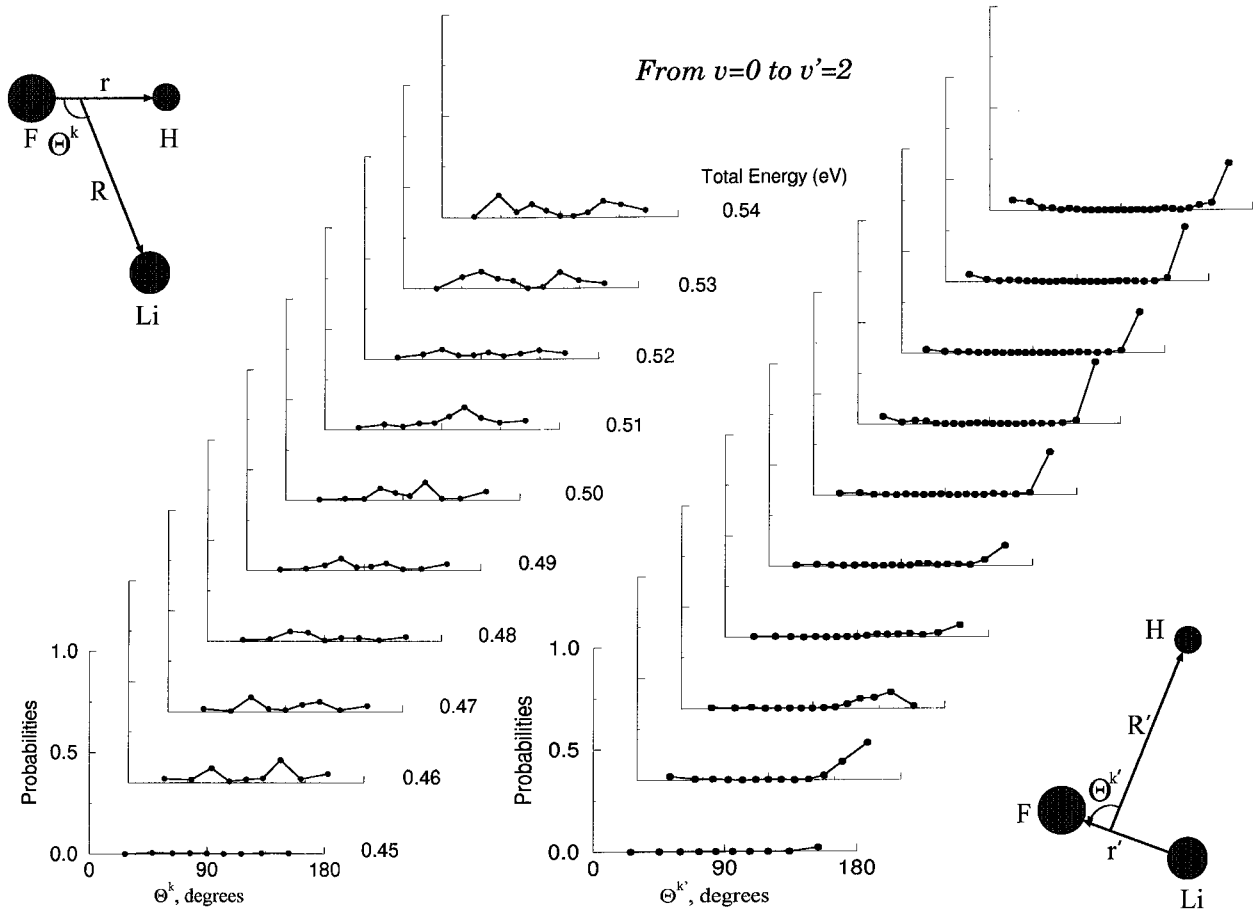


**Figure 5.** As in Figure 3, for Li + HF($v = 0$) → LiF($v' = 2$) + H.

probability matrix whose elements are $P^{J=0}_{\tau\tau'}(v \rightarrow v')$ as well as the quantities $P^{J=0}_{\tau\tau'}(v)$ and $P^{J=0}_{\tau\tau'}(v')$ obtained summing over $v'$ and $v$, respectively. For these calculations the zero total angular momentum **S** matrix elements computed using the hyperspherical formalism[34,35] for an interval of total energy values covering the range from 0.45 to 0.54 eV in steps of 0.01 eV were used. In this energy interval the reactant $v = 0$ and product $v' = 0$, 1, 2 vibrational states are open.

To carry out the RSD analysis, the $|jl\rangle$ representation of **S** was transformed into the helicity and stereodirected ones. Then the square modulus of individual elements were summed either over $v'$ or over $v$ to obtain $P^{J=0}_{\tau\tau'}(v)$ and $P^{J=0}_{\tau\tau'}(v')$, i.e., cumulative (though still state-specific) *steric effects.*

Results for the probability matrices $P^{J=0}_{\tau\tau'}(v \rightarrow v')$ at two collision energies and for the transition from $v = 0$ to $v' = 2$ are given in Figure 2 by plotting related contour maps. The figure shows that, in general, the **S** matrix is rather "sparse". Important probabilities accumulate only at the positive $v'$ edge. This indicates a large polarization effect for products, with the H atom separating preferentially within a narrow cone on the F side of the LiF molecule. The structure of the reactive probability, when this is plotted as a function of the reactant collision angle, is bimodal, whereas when the reactive probability is plotted as a function of the product collision angle, there is only one peak (corresponding to exits on the F side) that indicates a clear dynamical bias of this system. The bimodal structure has a peak at positive values of $v$ and a peak at negative values of $v$.

In Figures 3−5 we show angle-dependent probabilities $P^{J=0}_{\tau\tau'}(v)$ at $v = 0$ and $v' = 0$, 1, 2, respectively, at all the energies considered. Plots of $P^{J=0}_{\tau\tau'}(v)$ have been discussed in the literature for the first time in ref 33. They are given in terms of the angle of attack $\Theta^k$, obtained from $v$ through eq 7. All the plots show in general a prominent peak at small $\Theta^k$ values, confirming that the F side is the most favorite side for reactive attacks. They also show a second peak at large $\Theta^k$ values, indicating that a substantial fraction of reactive attacks take place from the H side. Such a structure becomes less pronounced when $v'$ increases.

The corresponding plots for the product arrangement are given on the right-hand sides of Figures 3−5 where $P^{J=0}_{\tau\tau'}(v')$ calculated at the different energies for the different $v'$ values are given. Again, irrespective of the amount of energy allocated as translation of the reactants, reactive events show a bias toward positive values of $v'$ meaning that the product atom is preferentially expelled by the F side. The globally nonmonotonic appearance of these plots is clear evidence of the highly quantum nature of this system.

## V. Conclusions

Different representations of the quantum **S** matrix can be used to derive information about the stereodynamics of an atom−diatom reaction. To this end, links between **S** matrix elements given in the helicity representation and both reactant and product polarizations can be established, as shown in the appendix section. Via a proper classical correspondence rule, multipole moments describing the polarization of a given angular momentum with respect to the direction of the cylindrical symmetry axis can be also linked to the value of the **S** matrix elements. In principle, all these quantities can be obtained from both physical and numerical (trajectory) experiments, allowing a crossed experimental−theoretical comparison. The complete

evaluation of all these quantities for the Li + HF reaction needs an extension of quantum calculations to large total angular momentum values; this is a very demanding computational task, presently being pursued.

The investigation has been extended here to exploit the advantage of using a stereodirected representation of the **S** matrix. This gave us the possibility of obtaining information on stereodynamical effects already from data calculated at zero total angular momentum. In particular, information was obtained on the preferred side of attack or the likely side of expulsion of the incoming or outgoing atom. This also allowed an analysis of the effect on the angular dependence of the reactivity of different allocations of energy among vibrational levels of both entrance and exit channels.

**Acknowledgment.** This work is supported by the European Union [TMR Network, Contract ERB-FMRX-CT96-0088] and as a part of the COST in Chemistry (D9 Action). It has also been financially supported by DGICYT of Spain (Grant PB95-0930) and MURST and CNR of Italy. T.M. thanks the Spanish Ministry of Education for a grant within the "Acciónes Integradas" scheme. V.A. and A.L. thank ZiF (Zentrum für Interdisziplinare Forschung, Universität Bielefeld) for hospitality during the work of the Forschungsgruppen on "Interactions of oriented molecules". J.M.A. thanks DGICYT of Spain for a sabbatical fellowship in Perugia (grant PR95-291).

## Appendix A: Stereodynamical Information from Helicity Representation

Although the focus in the main text was on the stereodirected representation, which deals with the role of angles of attack and recoil, in the helicity representation the **S** matrix elements are explicitly labeled by the rotational quantum numbers $j$ and $j'$. This representation is suited to the discussion of experimentally observable polarization effects, although this requires information, presently unavailable, also for $J > 0$. Vector correlations rich in information about the stereodynamics of atom−diatom chemical reactions are those concerning the entrance and exit relative velocity vectors **k** and **k′** and the rotational angular momenta **j** and **j′** for the reactant and product diatom arrangement, which will be denoted by $\tau$ and $\tau'$, respectively. Classically, the distributions of the polarization for reactant, $P_{\tau\tau'}(\hat{\mathbf{k}}\cdot\hat{\mathbf{j}})$, and for product, $P_{\tau\tau'}(\hat{\mathbf{k}}'\cdot\hat{\mathbf{j}}')$, are defined. These distributions can be easily obtained from trajectory calculations (see, for example, ref 36) and from experiments.[3] As far as quantum results are concerned, the $|j\Omega\rangle$ representation of the **S** matrix contains information related to these distributions. As already mentioned, in the helicity representation the discrete values of $\Omega$ quantize[29,30] the projection of **J** and **j** onto $\mathbf{R}_\tau$. Since in this frame the relative velocity **k** coincides with $\mathbf{R}_\tau$ (apart from a phase $\pi$), the $|j\Omega\rangle$ representation contains information about the $(\hat{\mathbf{k}}\cdot\hat{\mathbf{j}})$ vector correlation.

In order to compare classical and quantum results, we forge a link between the scattering matrix and the polarization distributions. The reaction probability from a reactant state labeled $v$, $j$, and $\Omega$ to a product state labeled $v'$, $j'$ and $\Omega'$, at a given total angular momentum $J$, is simply the squared modulus of the corresponding **S** matrix element:

$$P^J_{\tau\tau'}(vj\Omega\rightarrow v'j'\Omega') = |S^J_{\tau vj\Omega,\tau' v'j'\Omega'}|^2 \qquad \text{(A1)}$$

To keep the notation as simple as possible, in the following we do not specify vibrational and rotational state labels. Accordingly, the probability defined in the above equation will be denoted by $P^J_{\tau\tau'}(\Omega\rightarrow\Omega')$. At this point a comparison with standard $J$-averaged trajectory results is possible by performing first a sum over all $\Omega'$

$$P^J_{\tau\tau'}(\Omega) = \sum_{\Omega'} P^J_{\tau\tau'}(\Omega\rightarrow\Omega') \qquad \text{(A2)}$$

and then a weighted sum over $J$

$$P_{\tau\tau'}(\Omega) = (J_{\max}+1)^{-2}\sum_{J=\Omega}^{J_{\max}}(2J+1)P^J_{\tau\tau'}(\Omega) \qquad \text{(A3)}$$

where the total angular momentum varies between $\Omega$ and $J_{\max}$, the largest contributing value to the partial wave convergence. Since $\Omega$ assumes all possible integer values from 0 to $\min(j, J)$, when $J \geq j$, all the orientations of $j$ are allowed and when $J < j$, the projection $\Omega$ is bound by $J$ and only some orientations of $j$ are allowed. By summing up all the relevant contributions, one can recover the overall probability at fixed $\Omega$ value.

An explicit formulation of the $(\hat{\mathbf{k}}\cdot\hat{\mathbf{j}})$ correlation is worked out by invoking the semiclassical vector model of the angular momentum[37]

$$|\hat{\mathbf{k}}\cdot\hat{\mathbf{j}}| \Leftrightarrow \frac{\Omega}{j+1/2} \qquad \text{(A4)}$$

where $0 \leq \Omega \leq \min(J,j)$; see section II. This equation is obviously in agreement with the fact that in a three-particle system the diatom has no rotational polarization and angular distributions of **j** and **j′** rotational angular momenta are necessarily aligned with respect to the relative entrance **k** and exit **k′** velocities. Semiclassical analyses[38] and trajectory calculations[36,39] show this clearly, since they lead to nonnegligible values only for the even Legendre moments of the corresponding angular distributions. This alignment is a consequence of the conservation of parity under the inversion of all coordinates and pictorially can be envisaged as a manifestation of the irrelevance for reactivity of the molecular sense of rotation with respect to the approach or recoil direction. However, it has to be emphasized here that **j** or **j′** may well show an orientation with respect to the **k**−**k′** plane.[38]

The comparison between the classical polarization of the reactant $P_{\tau\tau'}(\hat{\mathbf{k}}\cdot\hat{\mathbf{j}})$ and the quantum transition probability $P_{\tau\tau'}(\Omega)$ is obtained through eq A4. As a result, from the complete set of **S** matrices at all $J$ values one can obtain the quantum mechanical $P_{\tau\tau'}(\Omega)$ distribution with a large (though discrete) collection of grid points. To the end result of comparing quasiclassical and quantum distributions, one can also bin the results and obtain histogrammic representations.

By exchanging in the given expressions $j$ and $\Omega$ with $j'$ and $\Omega'$, respectively, and going through similar considerations, we get the quantum mechanical counterpart, $P_{\tau\tau'}(\Omega)$, for the product polarization distribution $P_{\tau\tau'}(\hat{\mathbf{k}}\cdot\hat{\mathbf{j}})$.

In the following we show that eq A4 is also useful for comparing quantum results with the polarization parameters[27,37] $A_0^{(k)}$ obtainable from the experiment. To establish a link between $P_{\tau\tau'}(\Omega)$ and the polarization parameters, we exploit the relationship between $P_{\tau\tau'}(\hat{\mathbf{k}}\cdot\hat{\mathbf{j}})$ and $P_{\tau\tau'}(\Omega)$ as well as the relationship between $P_{\tau\tau'}(\Omega)$ and the different fixed $J$ contributions; see eq A3.

By enforcement of the cylindrical symmetry, explicit expressions in terms of the **S** matrix can also be derived for the $A_0^{(k)}(J)$ multipole moments describing the polarization of the considered angular momentum with respect to the quantization

axis and for their mean values $A_0^{(k)}$. Under the cylindrical symmetry constraint, the spherical-tensor angular momentum operators, which naturally appear in the stereodynamics of angular momenta, are functions of the more usual operators for the total angular momentum and its projection.[27,37] Following ref 37 (see p 234), we have worked out an expression for the main alignment parameter $A_0^{(2)}$

$$A_0^{(2)} = -1 + 3(J_{max} + 1)^{-2} \sum_{\Omega=0}^{\min(j,J)} \sum_{J=\Omega}^{J_{max}} (2J+1) \frac{\Omega^2}{(j+1/2)^2} P^J_{\tau\tau'}(\Omega) \quad \text{(A5)}$$

in terms of the reaction probabilities $P^J_{\tau\tau'}(\Omega)$ (see eq A2) at fixed $J$ and $\Omega$. This is the first non-null polarization parameter and can be compared with the experimental results and standard classical calculations.

From the above equation we can also derive an expression for the alignment parameter at fixed total angular momentum

$$A_0^{(2)}(J) = (J_{max} + 1)^{-2} \left[ -1 + 3 \sum_{\Omega} \frac{\Omega^2}{(j+1/2)^2} P^J_{\tau\tau'}(\Omega) \right] \quad \text{(A6)}$$

The above expressions can also be used to calculate the polarization parameter for the product arrangement using proper quantities. Higher multipole moments can be evaluated using a similar procedure. For a recent alternative to these quantities, closer to the spirit of the present paper, see ref 40, section IVB.

## References and Notes


(1) Aquilanti, V; Laganà, A.; Levine, R. D. *Chem. Phys. Lett.* **1989**, *158*, 87.

(2) Becker, C. H.; Casavecchia, P.; Tiedemann, P. W.; Valentini, J. J.; Lee, Y. T. *J. Chem. Phys.* **1980,** *73*, 2833.

(3) Loesch, H. J.; Stienkemeier, F. *J. Chem. Phys.* **1993,** *98*, 9570.

(4) Yang, C. Y.; Klippenstein, S. J.; Kress, J. D.; Pack, R. T; Parker, G. A.; Laganà, A. *J. Chem. Phys.* **1994**, *100*, 4917.

(5) Noorbatcha, I.; Sathyamurthy, N. *J. Am. Chem. Soc.* **1982**, *104*, 1766.

(6) Noorbatcha, I.; Sathyamurthy, N. *Chem. Phys.* **1982**, *76*, 6447.

(7) Noorbatcha, I.; Sathyamurthy, N. *J. Chem. Phys.* **1983**, *77*, 67.

(8) Noorbatcha, I.; Sathyamurthy, N. *Chem. Phys. Lett.* **1982**, *93*, 432.

(9) Alvariño, J. M.; Casavecchia, P.; Gervasi, O.; Laganà, A. *J. Chem. Phys.* **1981**, *77*, 6341.

(10) Laganà, A.; Hernández, M. L.; Alvariño, J. M. *Chem. Phys. Lett.* **1984**, *106*, 41.

(11) Alvariño, J. M.; Hernández, M. L.; Garcia, E.; Laganà, A. *J. Chem. Phys.* **1986**, *84*, 3059.

(12) Laganà, A.; Gimenez, X.; Garcia, E.; Aguilar, A.; Lucas, J. M. *Chem. Phys. Lett.* **1991**, *176*, 280.

(13) Baer, M.; Last, I.; Loesch, H. J. *J. Chem. Phys.* **1994,** *101*, 9648.

(14) Gögtas, F.; Balint-Kurti, G. G.; Offer, A. R. *J. Chem. Phys.* **1996**, *104*, 7927. Zhu, W.; Wang, D.; Zhang, J. Z. *Theor. Chem. Acc.* **1997**, *96*, 31.

(15) Parker, G. A.; Pack, R. T; Laganà, A. *Chem. Phys. Lett.* **1993**, *202*, 75.

(16) Parker, G. A.; Laganà, A.; Crocchianti, S.; Pack, R. T. *J. Chem. Phys.* **1995,** *102*, 1238.

(17) Carter, S.; Murrell, J. N. *Mol. Phys.* **1980,** *41*, 567.

(18) Laganà, A.; Gervasi, O.; Garcia, E. *Chem. Phys. Lett.* **1988**, *143*, 174.

(19) Palmieri, P.; Laganà, A. *J. Chem. Phys.* **1989,** *91*, 7302.

(20) Chen, M. M. L.; Schaefer, H. F., III. *J. Chem. Phys.* **1980,** *72*, 4376.

(21) Aguado, A.; Paniagua, M.; Lara, M.; Roncero, M. *J. Chem. Phys.* **1997,** *106*, 1013.

(22) Loesh, H. J. *Annu. Rev. Phys. Chem.* **1995**, *46*, 555. Loesch, H. J.; Remscheid, A.; Stenzel, E.; Stienkemeier, F. Wuestenbecker, B. In *Physics of Electronic and Atomic Collisions;* MacGillivray, W. R., McCarthy, I. E., Standage, M. C., Eds.; Adam Hilger: Bristol, 1992; p 579.

(23) Alvariño, J. M.; Basterrechea, F. J.; Laganà, A. *Mol. Phys.* **1986,** *59*, 559.

(24) Crocchianti, S. Ph.D. Thesis, Università di Perugia, Italy, 1997.

(25) Maltz, C.; Weinstein, N. D.; Herschbach, D. R. *Mol. Phys.* **1972**, *24*, 133.

(26) Case, D. A.; Herschbach, D. R. *Mol. Phys.* **1975,** *30*, 1537.

(27) Orr-Ewing, A. J.; Zare, R. N. *Annu. Rev. Phys. Chem.* **1994**, *45*, 315.

(28) de Miranda, M. P.; Clary, D. C. *J. Chem. Phys.* **1997**, *106*, 4509.

(29) Launay, J. M. *J. Phys. B: At. Mol. Phys.* **1976**, *9*, 1823.

(30) Aquilanti, V.; Cavalli, S.; Grossi, G.; Anderson, R. W. *J. Phys. Chem.* **1991**, *95*, 8184.

(31) Aquilanti, V.; Beneventi, L.; Grossi, G.; Vecchiocattivi, F. *J. Chem. Phys.* **1988,** *89*, 751.

(32) Aquilanti, V.; Grossi, G. *Lett. Nuovo Cimento* **1985,** *42*, 157. Aquilanti, V.; Cavalli, S.; Grossi, G. *Theor. Chim. Acta* **1991,** *79*, 283. Aquilanti, V.; Cavalli, S. *Few-Body Syst., Suppl.* **1992**, *6*, 573. Aquilanti, V.; Cavalli, S.; Monnerville, M. In *Numerical Grid Methods and Their Applications to Schrödinger Equation;* Cerjan, C., Ed.; Kluwer: Dordrecht, 1993; p 25. Aquilanti, V.; Cavalli, S.; De Fazio, D. *J. Phys. Chem.* **1995,** *99*, 15694. Aquilanti, V.; Cavalli, S.; De Fazio, D. *J. Chem. Phys.* **1998**, *109*, 3792. Aquilanti, V.; Cavalli, S.; De Fazio, D.; Volpi, A.; Aguilar, A; Gimenez, X.; Lucas, J. M. *J. Chem. Phys.* **1998**, *109*, 3805.

(33) Alvariño, J. M.; Aquilanti, V.; Cavalli, S.; Crocchianti, S.; Laganá, A.; Martinez, T. *J. Chem. Phys.* **1997**, *107*, 3339.

(34) Pack, R. T.; Parker, G. A. *J. Chem. Phys.* **1987,** *87*, 3888.

(35) Pack, R. T.; Parker, G. A. *J. Chem. Phys.* **1989**, *90*, 3511.

(36) Alvariño, J. M.; Laganà, A. *J. Chem. Phys.* **1991,** *95*, 998.

(37) See, for example, the following. Zare, R. N. *Angular Momentum: Understanding Spatial Aspects in Chemistry and Physics;* Wiley: New York, 1988. For the use of $j + 1/2$ rather than $(j(j+1))^{1/2}$, see ref 30.

(38) Aoiz, F. J.; Brouard, M.; Enriquez, P. A. *J. Chem. Phys.* **1996**, *105*, 4964.

(39) Alvariño, J. M.; Bolloni, A.; Hernandez, M. L.; Laganà, A. *J. Phys. Chem.*, in press.

(40) Aquilanti, V.; Ascenzi, D.; Cappelletti, D.; Fedeli, R.; Pirani, F. *J. Phys. Chem. A* **1997**, *101*, 7648.